**Article:**
Nwonu, D.C. and Onyia, M.E. (2023) Novel grey-vector optimization of desiccation-induced shrinkage and strength of industrial waste-based soil-composite binder as sustainable construction material. Journal of Material Cycles and Waste Management, 25 (4). pp. 2123-2134. ISSN: 1438-4957

https://doi.org/10.1007/s10163-023-01663-2

# NOVEL GREY-VECTOR OPTIMIZATION OF DESICCATION-INDUCED SHRINKAGE AND STRENGTH OF INDUSTRIAL WASTE-BASED SOIL COMPOSITE BINDER AS SUSTAINABLE CONSTRUCTION MATERIAL

**Donald Chimobi Nwonu[1]* and Michael Ebie Onyia[2]**

[12]*Civil Engineering Department, University of Nigeria Nsukka, 410001, Nsukka.*

[1]donald.nwonu@unn.edu.ng, and [2]michael.onyia@unn.edu.ng

[1]*Orcid ID: http://orcid.org/0000-0002-5106-4579*

**Correspondence*:** Donald Chimobi Nwonu; donald.nwonu@unn.edu.ng; +2348065345122

## ABSTRACT

Infrastructural development geared towards sustainable cities and communities requires the adoption of sustainable construction materials. As a contribution towards this, optimization of the unconfined compressive strength (UCS) and desiccation-induced shrinkage (DS) behavior of expansive soil stabilized with alkali-activated waste materials was executed. A novel approach was applied for the multiple characteristics optimization of the developed industrial waste-based soil-composite binder for use in construction. Laboratory experiments were done employing Taguchi design and considering several process parameters. The outcome of the single response optimization based on Taguchi signal–to–noise ratio (SN) analysis resulted in conflicting optimal levels for the UCS and DS. Hence, a novel multi-response optimization was applied to concurrently optimize the UCS and DS based on grey–vector analysis (GVA). The outcome of the GVA identified the greatest factor effects on the vector resultant to be waste quantity, type and preparation method. The new method was compared with the renowned Taguchi–grey relational analysis and was found to be more computationally efficient, in addition to matched performance based on Euclidean distance between the optimal solutions. Thus, the new method can serve construction engineers in development of alkali-activated waste–treated soil as sustainable construction material for embankments and waste containment.

**Keywords:** desiccation–induced shrinkage, grey–vector analysis, industrial wastes, optimization, unconfined compressive strength.

## Introduction

Expansive soils, which are widely distributed globally potentially constitutes an integral component of many civil engineering infrastructures such as roads, embankments, fills, buried pipelines, railways and waste containment facilities. Indeed, the utilization of such material in construction applications is clearly inevitable. Great concerns however, arise due to the adverse volume change orchestrated by the proliferation of moisture infiltration in contact with the soil, which causes severe distress to overlying infrastructure and other geo-structures. Instructively, this nature of expansive soils obviously encourages various mechanisms of infrastructure deterioration, one form of which is the renowned desiccation-induced shrinkage (DS) cracking.

Superficial and subterranean cracking of expansive clays resulting from desiccation effect on environmental exposure has been reported as the cause of various geo-hazards including failure of pavements, waste containment infrastructures, reservoirs, natural and engineered slopes [1, 2, 3, 4]. In the case of road pavements, macro-cracks constitute pathways for moisture infiltration and the subsequent loss of bearing strength of the subgrade layer that acts as the pavement foundation, ultimately resulting to pavement failure [4, 5, 6]. In waste containment infrastructures, desiccation – induced volumetric shrinkage leads to increment in the permeability of the liner material, which can permit leachate, mine tailings or other toxic wastes to find its way to the groundwater, in addition to the shear failure of engineered landfills [1, 8, 9]. Similarly, surficial slope failures occur due to cracks, which not only increases infiltration to increase pore water pressures, but also causes suction loss that ultimately results in shear strength attenuation with time [4, 10, 11]. These considerations therefore necessitate the adoption of sustainable technologies to mitigate the DS cracking of expansive soils, while improving strength for durability as a veritable construction material.

In this regard, various technologies have been experimented in recent years to improve expansive soils in a sustainable manner. This is often attempted by adopting the use of industrial waste materials, which not only serve as a soil improvement strategy, but also serves the complementary purpose of waste management. Several industrial wastes have been used in soil improvement, including rice husk ash, fly ash, quarry waste (QW), tailings, waste tires and others [12]. In the study by Ahmed and Naggar [13], basanite-tire waste mixtures were deployed to improve the strength of a silty soil. The results show that the addition of recycled basanite waste had a more positive effect on the compressive strength improvement, while the rubber tire waste increased the tensile resistance of the soil. In a related study [14], various percentages of waste marble powder additive (5, 10, 20, 30 and 50%) and curing time (0, 7, 30 and 60 days) were considered for soil strength improvement. The UCS of the uncured soil samples attained peak values at 5% marble waste content, whereas the cured specimens only showed strength gain at 7 days, which suggest a threshold for the occurrence of chemical reactions within the soil-additive matrix. The stabilized soil generally resisted freeze-thaw cycles up to the $5^{th}$ cycle before failure. It was also reported that mass loss increased with increase in the freeze-thaw cycles; however, for each cycle, the stabilized soil had lower mass loss in comparison with the untreated soil, indicating its durability for practical application. Other studies have similarly reported strength improvement with the addition of industrial waste materials [15, 16, 17, 18].

Instructively, these studies suggest that soils can be improved using industrial wastes, albeit the extent of improvement achievable is less when compared with the conventional materials such as cement and lime, which are considered to be eco-unfriendly. The search for a more robust technology birthed the utilization of geopolymer technology in soil improvement, which has comparative strength improvement with cement and lime, while maintaining eco-friendliness [19, 20]. Geopolymer soil stabilization has emerged in recent years in the area of soft ground improvement and has been widely reported. Murmu et al. [19] improved the properties of black clay using fly ash waste as geopolymer binder, considering different binder contents and curing ages (0, 7, 14, 28 and 90 days). The outcome of the study revealed that with increase in geopolymer content and curing time, the UCS and bearing strength of the soil significantly improved. The UCS increased from an initial value of about 200 kPa to an ultimate high of about 3250

kPa, while the bearing strength improved from 3% to about 42% under unsoaked condition. Furthermore in a similar study [21], the shrinkage limit of black clay was minimized from a value of about 32% to less than 1%. Similar studies have also shown that geopolymer soil stabilization using industrial waste materials significantly improves soils for various construction applications [22, 23, 24].

Previously, it has been reported that several process parameters influence the development of geopolymer binders for soft ground improvement, which necessitates the costly and time-consuming experimental trials [20, 25]. Thus, this motivates the search for robust optimization approaches for their development. Taguchi method has shown to be the preferred and reliable method so far and is typically opted for in the robust development of geopolymers for construction applications [26, 27, 28]. However, the Taguchi method can only optimize responses singly and hence; a multi-response technique has to be integrated into it for the concurrent optimization, which inspired a novel aspect of the present study.

In the present study, geopolymer binders based on industrial wastes including QW and palm oil fuel ash (PFA) were used to minimize the DS of an expansive soil while maximizing the UCS, adopting the Taguchi method. The novel highlight of this study showcases an optimization method, which has been developed from the simple concept of vector analysis. Furthermore, a comparative analysis is conducted with a renowned multi-response method based on grey relational analysis (GRA), and the advantages of the new method have been emphasized.

## Optimization Background

### Taguchi method

Design of experiment that is based on the Taguchi method is a renowned robust approach for product development. The method employs the use of orthogonal arrays, which ensures that the experimental space is navigated in a balance manner to achieve an optimized product [29]. Moreover, the signal-to-noise ratio (SN) optimization function is used to ensure minimum deviation from a specified target to ascertain the overall quality of the product development process [29]. These unique attributes, make the Taguchi method a very simple and reliable method for industrial product development. Lately, ample applications of the method have been reported in different ground improvement schemes for single response optimization [29, 30, 31]. Thus, it is a highly favored method for the construction industry in single response scenarios.

On the other hand, when multiple responses are involved, other multi-response methods have to be integrated with the Taguchi method. Some of these methods include genetic algorithm weighting, GRA, data envelopment analysis, utility concept, to mention but a few. More often than not, in addition to the issue of lack of distinctiveness in the optimal solution; these methods require great computational effort and are often based on advanced analytical or numerical approaches, which make them inapt for direct practical use [7, 32]. For instance, in the analytical method based on GRA, several computations are required for the multi-response attribute known as grey relational grade (GRG). These computations include: comparability sequence (grey relational generation), deviation sequence, grey relational coefficients and then the GRG. Moreover, a weighting factor, which is more commonly denoted as the identification

coefficient, $\zeta$ is required for weighting the prioritization of each multiple attribute [33]. As such, various methods are adopted for its selection namely intuitionist approach, entropy weighting method, analytic hierarchy process, et cetera. This further compounds the GRA and could introduce bias depending on the level of subjectivity inherent in the adopted response prioritization method. This challenge is similarly shared by other multiple response methods such as the utility concept [28]. Apparently, there is need for improved techniques that will surmount the aforementioned drawbacks associated with Taguchi multi-response optimization. In view of this, a new approach is proposed in the present study.

**Proposed grey-vector analysis**

In this study, a method is presented, which is based on the processes of grey-based normalization and vector analysis. In an orthogonal array experiment, each individual response data representing the quality attributes of a product is obtained as a $n \times 1$ vector. Instructively, this data is rightly a vector since it has magnitude and a direction, which is defined by the optimization objective. As such, it is amenable for vector analysis using algebra of vectors. Since the concurrent attainment of the desired optimum is required for the product development, the concurrent effect of all the vectors representing the quality attributes is determined. In vector physics, this overall effect of vectors is known as the resultant vector, $\mathrm{R}$ and can be expediently obtained from vector algebra. The method proposed in the present study is mathematically represented thus:

Consider a product, in which the overall quality $Y$ is based on $X_k$ attributes defined as the function in Equation 1.

$$Y = f(X_1, X_2, \dots, X_k) \tag{1}$$

Each $X_i$ attribute is considered as a $n \times 1$ vector representing the product's experimental data space, while the overall product quality is also represented as a $n \times 1$ vector. Hence, Equation 1 is aptly represented in vector notation as shown in Equation 2.

$$\vec{Y} = f\left(\overrightarrow{X_1}, \overrightarrow{X_2}, \dots, \overrightarrow{X_k}\right) \tag{2}$$

The quantities representing each $ith$ row entry of the $X_j$ column are the scalar elements for each vector, which defines the magnitude, while the optimization objective defines the vector direction. These scalar elements are the normalized SN, known as the comparability sequence. Thus, the analytical function that defines the overall effect of each component vector is the resultant vector. This resultant represents the overall multi-characteristics quality attribute, $Y$ and can be expressed as the sum of each vector component as shown in Equation 3, based on a priori definitions explained subsequently.

$$\vec{Y} \equiv \vec{\mathrm{R}} = \sum_{j=1}^{k} \overrightarrow{X_j}$$

(3)

In order to assuage bias towards vectors of higher magnitude, grey normalization is applied on the data prior to the vector analysis. The min-max grey normalization functions are shown in Equations 4 and 5 for the respective minimization and maximization objectives.

$$\eta_i^*(j) = \frac{max\ \eta_i^0(j) - \eta_i^0(j)}{max\ \eta_i^0(j) - min\ \eta_i^0(j)}$$

(4)

$$\eta_i^*(j) = \frac{\eta_i^0(j) - min\ \eta_i^0(j)}{max\ \eta_i^0(j) - min\ \eta_i^0(j)}$$

(5)

Where $\eta_i^0(j)$ is the base sequence, which represents the SN; $min\ \eta_i^0(j)$ and $max\ \eta_i^0(j)$ are taken as the respective minimum and maximum of the sequence (that is min and max of SN); $\eta_i^*(j)$ is then the comparability sequence, which represents the normalized SN.

The SN for the respective minimization and maximization respectively denoted as smaller-the-better (STB) and higher-the-better (HTB) functions are given as shown in Equations 6 and 7.

$$\eta = -10log_{10}\left(\frac{1}{n}\sum_{i=1}^{n}(X_i + X_0)^2\right)$$

(6)

$$\eta = -10log_{10}\left(\frac{1}{n}\sum_{i=1}^{n}\left(\frac{1}{X_i + X_0}\right)^2\right)$$

(7)

Where the number of response data per experimental run is $n$, $X_i$ is the response value and $X_0$ is the target value. In the case of the HTB and STB SN, the unstated target is zero.

It is noteworthy at this juncture that Equation 3 holds as long as the SN functions are used. This is true because an implicit requirement of Equation 3 is that all the $\overrightarrow{X_j}$ have the same direction, which is attainable for SN functions that

are always maximized. Hence, when SN is used, the vector directions are the same. In contrast, when the individual responses require either of minimization or maximization, the appropriate vector resultant function has to be used in Equation 3 since the vector directions differ in an opposing manner. Similarly, Equation 5 must be used with the SN; else, either of Equations 4 or 5 should be employed for the respective minimization or maximization objective. However, the SN functions are strongly recommended for use to prevent computation errors and ensure a robust optimization design. The final optimization Equation is represented in Equations 8-9.

Maximize:

$$\vec{\mathrm{R}} = \sum_{j=1}^{k} \overrightarrow{X_j} \tag{8}$$

Subject to

$$0 \leq \eta_i^*(j) \leq 1 \quad \forall \overrightarrow{X_j^k} \tag{9}$$

The overall product quality is thus obtained from the optimization shown in Equations 8-9 taking the resultant function to be the HTB SN function.

**Methodology**

**Materials**

The data used in the present study is based on the Taguchi-based experiment conducted by Nwonu [35] for the development and application of expansive soil geopolymer binders. In the study by Nwonu [35], a locally sourced expansive soil with geotechnical properties as shown in Table 1 was treated with alkali-activated binders made from two industrial waste materials QW and PFA. These waste materials were also sourced locally from their point of disposal and were then characterized to obtain their chemical oxide composition summarized in Table 2.

**Laboratory experiments**

Laboratory experiments were conducted to determine the UCS and DS of the alkali-activated treated samples as reported by Nwonu [35]. The UCS test was conducted in a compression testing machine based on the specifications of the British standard institute. The tested samples were initially compacted in the laboratory based on the British standard light compactive energy at the required moisture content and then cured for 7 days under humidity controlled condition for strength development. The required moisture content was obtained from the moisture density

relationship for the geopolymer mixtures, which was generally within the optimum moisture content for the natural soil 19.7 ± 2% as reported in previous study [9]. The compaction was done in the standard Proctor mold, after which cylindrical 38 mm diameter by 76 mm height specimens were extruded for the UCS test.

The DS test was conducted as per previous studies [36, 37]. The samples were prepared at the required moisture content using the previously described compaction method. Then, three cylindrical specimens of 38 mm diameter by 76 mm height were extruded from the compaction mold. The cylinderical specimens were allowed to air-dry on the laboratory bench in order to closely simulate the in situ environmental condition. At least, three measurements of the height and diameter were taken using a vernier calliper until there was no further reduction in mass, representing no further moisture loss. The average measurements were used to compute the final volume and determine the volumetric shrinkage, which is the DS in this study.

**Experimental design and optimization**

The aforedescribed laboratory experiments were performed based on a designed experiment by Nwonu [35], empoying the L8 Taguchi orthogonal array. The process parameters considered were the waste type (factor A), waste content (factor B), activator type (factor C), ratio of activator to waste content on mass basis (factor D) and method of mixing (factor E). the two levels used in factor C are the sodium hydroxide (NaOH) and potassium hydroxide (KOH), while two mixing methods M1 and M2 were used. In M1, the soil and industrial wastes were homogenously mixed before the activator was added, whereas in M2, the activator and industrial waste were mixed prior to adding to the soil. The alkali-activator comprised of an equal amount of alkali hydroxide and water glass. The factors and their two-level designations are shown in Table 3, while the orthogonal array containing both the coded and uncoded variables is shown in Table 4 along with the obtained SN. The SN was obtained for the UCS using HTB fuction for maximization, whereas that of the DS was computed using the STB for minimization.

The flow charts for the GVA and the GRA used for the multi-response optimization are clearly presented in Figs 1 and 2 respectively. It is clear that the GVA is more computationally efficient because it requires less computation processes than the GRA for the multi-response optimization.

**Results & Discussion**

**Individual response optimization**

Assessment of the effect of process factors on the DS is clearly shown in the SN plot of Fig 3. It can be seen that factors E, A and B have the most significant effect on the variation of the DS based on the magnitude of the difference in SN between the factor levels. Apparently, the method of soil stabilization that involves mixing the industrial waste with the soil prior to alkaline activation is more effective for the reduction of the DS. Furthermore, the choice of PFA as a preferable industrial waste for DS minimization is also inferred. Moreover, the use of a higher percentage (20%) of the industrial waste gives a better improvement in the DS behavior of the soil. These factors are very pertinent in achieving a stabilized soil with minimum DS. Based on the Taguchi SN analysis, the optimal factor levels is obtained

from Fig 3 as A1 – B2 – C2 – D1 – E1. Using this optimal, the predicted DS based on the Taguchi additive model is 1.1% (SN = -8.849). This represents a tremendous reduction in the DS of the soil from an initial value of 20.3%, which demonstrates the stabilization capability of the alkali-activated additive used in the present study.

In a related development, a similar representation of the factor effects on the UCS of the stabilized soil is displayed in Fig 4. The factors B and C clearly had the most significant influence on the soil strength behavior. This implies that the quantity of the industrial waste and the alkali type have notable effect on the strength development of the stabilized soil. The potassium-based activator appears to give an improved soil of higher strength than the sodium-based activator. The possible underlying mechanisms which are responsible could be similarly attributed to the effect of moisture content on the ionic changes which occur at the diffuse double layer of the expansive clay [9]. This causes significant modifications in the strength of the bonds at the interlayer, which is dependent upon the nature of the ions in contact with the diffuse double layer of the soil within the clay-pore fluid media. The optimal factor level as shown by the maximum SN in Fig 4 corresponds to A2 – B2 – C1 – D2 – E1. The predicted UCS value obtained at this optimum using the Taguchi additive model is 489. 25 kN/m$^2$ (SN = 54.206). This represents a huge increment of about 276% in the UCS of the stabilized soil.

Despite these significant improvements in the DS and UCS of the soil achieved via alkali-activation, it is also noteworthy that the optimal levels for factors A, C and D are conflicting. This presents a dilemma to the mix design engineer charged with the responsibility of prescribing the optimum mixing method in field application. To resolve this identified conflict, further analysis was executed using the novel method developed in the present study and is explicitly presented in the subsequent section.

**Grey-vector analysis multi-response optimization**

The outcome of the novel GVA executed for the multi-response optimization of the DS and UCS using the steps shown in Fig. 1 produced the result summarized in Table 5. Determination of the factor effects on the Taguchi SN computed using the HTB function due to the desirability of higher resultant produced the results shown in Fig. 5 and Table 6. The Figure clearly shows that the factors which had the most significant effect on the vector resultant are A, B, and E. The extent of their effect on the vector resultant can be summarized in descending order as B > E >A > D > C as can be clearly observed from Table 6.

Furthermore, analysis of variance (ANOVA) was conducted by computation of the sum of squares (SS), mean squares (V), variance ratio (F-ratio) and percentage contribution (P), taking into account the degrees of freedom (DOF) of each process parameter [29]. The result, which is summarized in Table 7 presents a quantitative assessment of the factor effects and is found to be consentient with the Taguchi analysis. It can be seen that the factor B contributed the most to the vector resultant variation with 41%, followed by factor E (38.5%) and then A (10.4%). Factors C and D have very negligible contribution to the variation of the vector resultant.

Apparently, a higher quantity of the industrial waste is needed to minimize the DS of the expansive soil, while maximizing the UCS. This reveals the high degree of waste reuse inherent in the geopolymer technology utilized in

the present study for the expansive soil improvement. Furthermore, it is pertinent to apply the correct preparation method for field application. Vividly, the result of the present study show that homogenously mixing the soil and industrial waste material prior to alkali-activation produces a stabilized soil of higher strength and minimized DS. Furthermore, the choice of PFA as a better industrial waste material for the soil improvement process has also been shown and is largely attributed to its large alumino-silicate content anticipated to be more amorphous than that of the QW. Therefore, future studies can explore the pretreatment of the QW (for instance heat treatment) to derive a more amorphous alumino-silicate framework before use.

Furthermore, to obtain the predicted optimum values of the DS and UCS, the optimal factor levels in Fig. 5, which is given as A1 – B2 – C1 – D2 – E1 is used for the response prediction. The optimum predicted DS is 1.85%, while that of the UCS is 458 kN/m$^2$. To verify the accuracy of the obtained optimum value, 90% confidence interval of the confirmation experiment was computed with Equation 10 [28].

$$CI = \pm \sqrt{F_{\alpha}(1, f_e) V_e \left[\frac{R + N_{eff}}{RN_{eff}}\right]} \tag{10}$$

Where $F_{\alpha}(1, f_e)$ is the F-ratio at confidence level of $1 - \alpha$ against DOF 1 and error DOF, $f_e$; R is the sample size for the confirmation experiment and $N_{eff} = N/1 + DOF_u$; $V_e$ is the error variance; N is the total number of trials, and $DOF_u$ is the total degrees of freedom associated with the estimate of the vector resultant value

The predicted optimum vector resultant, is given as $2 \pm 0.5895$. The obtained SN from the confirmatory experiments for the respective DS and UCS were -4.7106 and 53.9794. Similarly, their vector resultant was gotten using Fig. 1, including the predicted and confirmatory experimental values in the comparability sequence of the orthogonal array. The computed vector resultant is 1.977, which is lucidly within the confidence interval of $2 \pm 0.5895$; hence, the prediction accuracy is verified.

**Comparative analysis of the novel GVA and GRA**

Multi-response optimization using GRA as applied in soil stabilization [38] is pertinent for comparison with the novel GVA. The required computations done for the GRA are summarized in Table 8, showing the comparability sequence, deviation sequence, grey relational coefficient, GRG and grey ordinal value (GOV) by applying the sequence in Fig.2. The factor effects are shown in Fig 6, which suggests the existence of two optimum solutions. The first solution is given as A1 – B2 – C2 – D2 – E1, while the second solution is A2 – B2 – C2 – D2 – E1. The predicted optimum for UCS and DS obtained with the first solution are 364.25 kN/m2 and 1.275% while that of the second solution gave UCS of 366 kN/m3 and DS of 3.7%. Rationally, the first solution is a better multi-response compromise to the single response optimization solution and thus was used further in the comparative analysis.

Confidence interval for the confirmatory experiment was similarly obtained using Equation 10. The predicted optimum solution was also verified at the 90% confidence interval of the confirmatory tests. In order to execute a direct comparison of the aptness of the compromise solution gotten using both GVA and GRA, a new approach was adopted in the present study by consideration of the Euclidean distance between the single response optimization solution (ideal solution) and each of the obtained multi-response optimization solution (compromise solution). The Euclidean distance is a robust approach, which is typically used as a similarity index measure in hierarchical cluster analysis [20], as well as in machine learning such as K-nearest neighbors. The general formula for the computation as applicable in the comparison of the optimization solutions is provided in Equation 11.

$$\Delta = \left[\sum_{j=1}^{k}\left(\eta_s^j - \eta_m^j\right)^2\right]^{\frac{1}{2}} \tag{11}$$

Where the Euclidean distance is $\Delta$, $\eta_s^j$ is the grey-based normalized single response predicted value for the $jth$ response and $\eta_m^j$ is the grey-based normalized multi-response predicted value for the $jth$ response.

It is noteworthy that the normalized responses are used in Equation 11 to resolve any inherent bias in responses of large magnitude. The grey-based normalization is executed using a comparability sequence comprised of the single response predicted values and all the multi-response solutions involved in the comparison. The outcome of this analysis is summarized in Table 9. The result clearly reveals the introduction of bias in the raw Euclidean distance computed using the non-normalized response. On the other hand, the normalized Euclidean distance clearly shows that the two multi-response methods exhibit a matched performance in their predicted optimum values. In a related development, the optimal solution obtained from the GVA is the same with that obtained using the utility concept [39] for the main effects. The upshot of this study also highlights the issue of non-uniqueness in the optimal solution for multi-response methods and is an aspect that requires further attention to create room for improvement. However, the GVA method developed in the present study is more computationally efficient than both GRA and the utility concept, because it requires fewer computations for multi-response optimization.

**Microstructural analysis of geopolymer structure**

Evidence of geopolymerization from the alkali-activation of alumino-silicate rich industrial waste materials can be revealed via microstructural analysis. The results of Fourier transform infrared spectroscopy (FTIR) and energy dispersive spectrophotometer elemental (EDSE) analysis are presented for the natural soil and the optimally stabilized soil in the respective Table 10 and Table 11, Fig 7.

The significant peaks for the natural soil from FTIR analysis show the presence of weakly bonded water molecules, typically expected within the clay-pore fluid media of expansive soils. Furthermore, peaks for inactive sites of alumino-silicate and quartz are present due to the crystalline nature of the alumino-silicate content of the natural soil,

in addition to the presence of significant amount of quartz mineral in the soil. The stabilized soil exhibited nuances, which give an indication of the occurrence of geopolymerization in the stabilized soil. The peaks for the water molecules slightly dropped to lower wave numbers, became broad, and sharp as presented in previous study [28]. These suggest that the water molecules have become strongly bonded. This is likely attributed to the stronger –OH bonding anticipated from the alkali activator [28, 39]. The inactive sites occurring in the stabilized soil could likely have resulted from that in the natural soil and some residual industrial waste particles in the stabilized soil matrix. Further indication of the geopolymerization reaction is provided by the carbonate functional group due to reaction of atmospheric $CO_2$ with the alkali activator (KOH) during mixing to form $K_2CO_3$ [28, 40]. The occurrence of the alumino-silicate gel band associated with the T–O sialate and siloxo framework confirms the formation of geopolymer binders in the stabilized soil [41, 42, 43].

Furthermore, the EDSE in Figure 7a show that the major elements prominent in the natural soil are Si, Al and Fe, based on the peaks. The atomic concentration of the elements is also shown in Table 11. This is as expected due to the rich content of the oxides of Si, Al and Fe in the oxide composition of the natural soil (Table 2). The stabilized soil EDSE peak show slight variation in the prominence of relevant elements in the soil. The peak for Al slightly dropped, while the peaks for Na and K became more prominent. These nuances are attributed to the formation of more siloxo alumino-silicate framework structures; in addition to the contributions of the sodium-based water glass ($Na_2SiO_3$) and potassium hydroxide (KOH) activator used for the alkali-activation.

**Conclusion**

Sustainable and improved construction materials are attainable by harnessing the reuse of industrial waste materials. This has been shown in the present study via the adoption of alkali-activation of PFA and QW for the improvement of the DS and UCS of an expansive soil. A robust and systematic experimental design and novel multi-response optimization approach was further adopted to ensure a replicable process when considered for field application. The developed composite material achieved very low volumetric DS (less than 4%) and high UCS value (far above 200 kPa) and can be employed as a sustainable construction material in embankments and waste containment facilities. The following summarizes the key findings of this study.

1. The key process factors which significantly influence the DS and UCS of the stabilized expansive soil using alkali-activated waste materials are the industrial waste quantity, method of preparation and waste type.
2. A computationally efficient novel multi-response optimization for the DS and UCS of the stabilized soil was developed based on grey normalization and vector analysis (GVA).
3. The optimally stabilized soil based on the GVA predicted significant improvement in the UCS (from 130 to 458kPa) and DS (from 20.3 to 1.85%). Moreover, the prediction was verified to be accurate at 90% confidence interval of the confirmation experiments.
4. The multi-response optimization and prediction using the novel GVA matched the performance of GRA based on the computed Euclidean distance between the single response prediction (ideal solution) and

multi-response prediction (compromise solution). In addition, the GVA gave the same optimization solution as the utility concept.

5. The GVA is regarded to be particularly advantageous, more desirable and expedient for construction and mix design engineers because it requires less computational effort than other multi-response methods.
6. Evidence of the geopolymerization process achieved via alkali-activation was confirmed based on FTIR and EDSE analysis, which revealed the formation of alumino-silicate gels in the stabilized soil.

**Declaration of Interest Statement**

The authors declare that there is no known conflict of interest associated with this study.

**References**


[1] J. L. Coo, Z. P. So and C. W. Ng, "Effect of nanoparticles on the shrinkage properties of clay," *Engineering Geology,* vol. 213, pp. 84-88, 2016.

[2] M. Sawada, Y. Sumi and M. Mimura, "Measuring desiccation-induced tensile cracking process," *Soils and Foundations,* 2021.

[3] R. A. Stirling, S. Glendinning and C. T. Davie, "Modelling the deterioration of the near surface caused by drying induced cracking," *Applied Clay Science,* vol. 146, pp. 176-185, 2017.

[4] C. S. Tang, B. Shi, C. Liu, L. Gao and H. I. Inyang, "Experimental investigation of the desiccation cracking behavior of soil layers during drying," *Journal of Materials in Civil Engineering,* vol. 23, no. 6, pp. 873-878, 2011.

[5] A. Soltani, A. Taheri, M. Khatibi and A. R. Estabragh, "Swelling potential of a stabilised expansive soil: A comparative experimental study," *Geotech Geol Eng,* 2017.

[6] D. C. Nwonu and C. C. Ikeagwuani, "Evaluating the effect of agro-based admixture on lime-treated expansive soil for subgrade material," *International Journal of Pavement Engineering,* pp. 1-15, 2019.

[7] C. C. Ikeagwuani and D. C. Nwonu, "Application of fuzzy logic and grey based Taguchi approach for additives optimization in expanisve soil treatment," *Road Materials and Pavement Design,* 2020.

[8] M. J. Ghazizade and E. Safari, "Analysis of desiccation crack depth in three compacted clay liners exposed to annual cycle of atmospheric conditions with and without a geotextile cover," *Journal of Geotechnical and Geoenvironmental Engineering,* vol. 143, no. 3, pp. 06016024-1-6, 2017.

[9] M. E. Onyia, J. C. Agunwamba and D. C. Nwonu, "Hydraulic conductivity behaviour of expansive soil geopolymer binders," *Arabian Journal of Geosciences,* vol. 14:503, 2021.

[10] S. Qi and S. K. Vanapalli, "Hydro-mechanical coupling effect on surficial layer stability of unsaturated expansive soil slopes," *Computers and Geotechnics,* vol. 70, pp. 68-82, 2015.

[11] C. C. Ikeagwuani and D. C. Nwonu, "Infuence of dilatancy behavior on the numerical modeling and prediction of slope stability of stabilized expansive soil slope," *Arabian Journal for Science and Engineering,* 2021.

[12] C. C. Ikeagwuani and D. C. Nwonu, "Emerging trends in expansive soil stabilisation: A review," *Journal of Rock Mechanics and Geotechnical Engineering,* vol. 11, pp. 423-440, 2019.

[13] A. Ahmed and M. H. Naggar, "Effect of cyclic loading on the compressive strength of soil stabilized with bassanite - tire mixture," *J Mater Cycles Waste Manag,* vol. 20, pp. 525-532, 2018.

[14] K. Aydin, O. Sivrikaya and F. Uysal, "Effects of curing time and freeze-thaw cycle on strength of soils with high plasticity stabilized by waste marble powder," *Journal of Materials Cycle and Waste Management,* 2020.

[15] N. Ural, C. Karakurt and T. Comert, "Influence of marble wastes on soil improvement and concrete production," *J Mater Cycles Waste Manag,* vol. 16, pp. 500-508, 2014.

[16] A. Srivastava, S. Pandey and J. Rana, "Use of shredded tire waste in improving the geotechnical properties of expansive black cotton soil," *Geomechanics and Geoengineering: An International Journal,* vol. 9, no. 4, pp. 303-311, 2014.

[17] M. Shahbazi, M. Rowshanzamir, S. M. Abtahi and S. M. Hejazi, "Optimization of carpet waste fibres and steel slag particles to reinforce expansive soil using response surface methodology," *Appl Clay Sci,* vol. 142, no. 15, pp. 185-92, 2017.

[18] D. C. Nwonu and C. C. Ikeagwuani, "Microdust effect on the physical condition and microstructure of tropical black clay," *International Journal of Pavement Research and Technology,* vol. 14, pp. 73-84, 2021.

[19] A. L. Murmu, N. Dhole and A. Patel, "Stabilisation of black cotton soil for subgrade application using fly ash geopolymer," *Road Materials and Pavement Design,* vol. 21, no. 3, pp. 867-885, 2020.

[20] D. C. Nwonu and C. N. Mama, "Delineating the aptness of improved geomaterial strength for ground improvement through microstructure and cluster analysis," *Indian Geotechnical Journal,* 2021.

[21] A. L. Murmu, A. Jain and A. Patel, "Mechanical properties of alkali activated fly ash geopolymer stabilized expansive clay," *KSCE Journal of Civil Engineering,* vol. 23, no. 9, pp. 3875-3888, 2019.

[22] P. Sukmak, S. Horpibulsuk and S. L. Shen, "Strength development in clay-fly ash geopolymer," *Construction and Building Materials,* vol. 40, pp. 566-574, 2013.

[23] H. Y. Leong, D. L. Ong, J. G. Sanjayan and A. Nazari, "Strength development of soil-fly ash geopolymer: Assessment of soil, flyash, alkali activators, and water," *Journal of Material in Civil Engineering,* vol. 30, no. 8, p. 04018171, 2018.

[24] M. Yaghoubi, A. Arulrajah, M. M. Disfani, S. Horpibulsuk, W. M. Bo and S. Darmawan, "Effects of industrial by-product based geopolymers on the strength developemnt of a soft soil," *Soils and Foundations,* vol. 58, pp. 716-728, 2018.

[25] D. C. Nwonu, "Exploring soil geopolymer technology in soft ground improvement: a brief excursion," *Arabian Journal of Geosciences,* vol. 14:460, pp. 1-20, 2021.

[26] M. Olivia and H. Nikraz, "Properties of fly ash geopolymer concrete designed by Taguchi method," *Mater Des,* vol. 36, pp. 191-198, 2012.

[27] A. Bagheri and A. Nazari, "Compressive strength of high strength class C fly ash-based geopolymers with reactive granulated blast furnace slag aggregates designed by taguchi method," *Materials & Design,* vol. 54, pp. 483-490, 2014.

[28] J. C. Agunwamba, M. E. Onyia and D. C. Nwonu, "Development of expansive soil geopolymer binders for use in waste containment facility," *Innovative Infrastructure Solutions,* vol. 6, no. 32, 2021.

[29] R. K. Roy, Design of experiments using the Taguchi approach; 16 steps to product and process improvement, New York: John Wiley & Sons. Inc, 2001.

[30] A. Kumar and D. K. Soni, "Effect of calcium and chloride based stabilizer on plastic properties of fine grained soil," *International Journal of Pavement Research and Technology,* vol. 12, pp. 537-545, 2019.

[31] B. Lafifi, A. Rouaiguia and N. Boumazza, "Optimization of geotechnical parameters using Taguchi's design of experiment (DOE), RSM and desirability function," *Innovative Infrastructure Solutions,* vol. 4:35, pp. 1-12, 2019.

[32] H. M. Bak, A. M. Halabian, H. Hashemolhosseini and M. Rowshanzamir, "Axial response and material efficiency of tapered helical piles," *Journal of Rock Mechanics and Geotechnical Engineering,* vol. 13, pp. 176-187, 2021.

[33] C. C. Ikeagwuani and D. C. Nwonu, "Multi-additive optimization for expansive soil treatment using grey-super-efficiency model integrated in Taguchi method," *Indian Geotechnical Journal,* 2021.

[34] J. Kundu and H. Singh, "Friction stir welding: multi-response optimisation using Taguchi-based GRA," *Production & Manufacturing Research,* vol. 4, no. 1, pp. 228-241, 2016.

[35] D. C. Nwonu, "Development and application of expansive soil geopolymer binders," Unpublished MEng. Thesis, University of Nigeria Nsukka, Nsukka, 2020.

[36] D. E. Daniel and Y. K. Wu, "Compacted clay liners and covers for arid sites," *Journal of Geotechnical Engineering,* vol. 119, pp. 223-237, 1993.

[37] K. J. Osinubi and C. M. Nwaiwu, "Design of compacted lateritic soil liners and covers," *Journal of Geotechnical and Geoenvironmental Engineering,* vol. 132, pp. 203-213, 2006.

[38] C. C. Ikeagwuani, J. C. Agunwamba, C. M. Nwankwo and M. Eneh, "Addtives optimization for expansive soil subgrade modification based on Taguchi grey relational analysis," *Internation Journal of Pavement Research and Technology,* 2020.

[39] X. Guo and Y. Wu, "Characterizing molecular structure of water adsorbed by cellulose nanofiber film using in situ micro-FTIR spectroscopy," *Journal of Wood Chemistry and Technology,* 2017.

[40] S. Pourakbar, A. Asadi, B. K. Huat, N. Cristelo and M. H. Fasihnikoutalab, "Application of alkai-activated agro-waste reinforced with Wallastonite fibers in soil stabilization," *J Mater Civ Eng,* p. 04016206, 2016.

[41] M. Criado, A. Palomo and A. Fernandez-Jimenez, "Alkai activation of fly ashes. Part 1: Effect of curing conditions on the carbonation of the reaction products," *Fuel,* vol. 84, pp. 2048-2054, 2005.

[42] S. S. Nenadovic, L. M. Kljajevic, M. A. Nesic, M. Z. Petkivic, K. V. Trivunac and V. B. Pavlovic, "Structure analysis of geopolymers synthesized from clay originated from Serbia," *Env Earth Sci,* vol. 76:79, 2017.

[43] L. K. Sharma, N. N. Sirdesai, K. M. Sharma and T. N. Singh, "Experimental study to examine the independent roles of lime and cement on the stabilization of a mountain soil," *Applied Clay Science,* vol. 152, pp. 183-195, 2017.

List of Tables

List of Figures

Figure

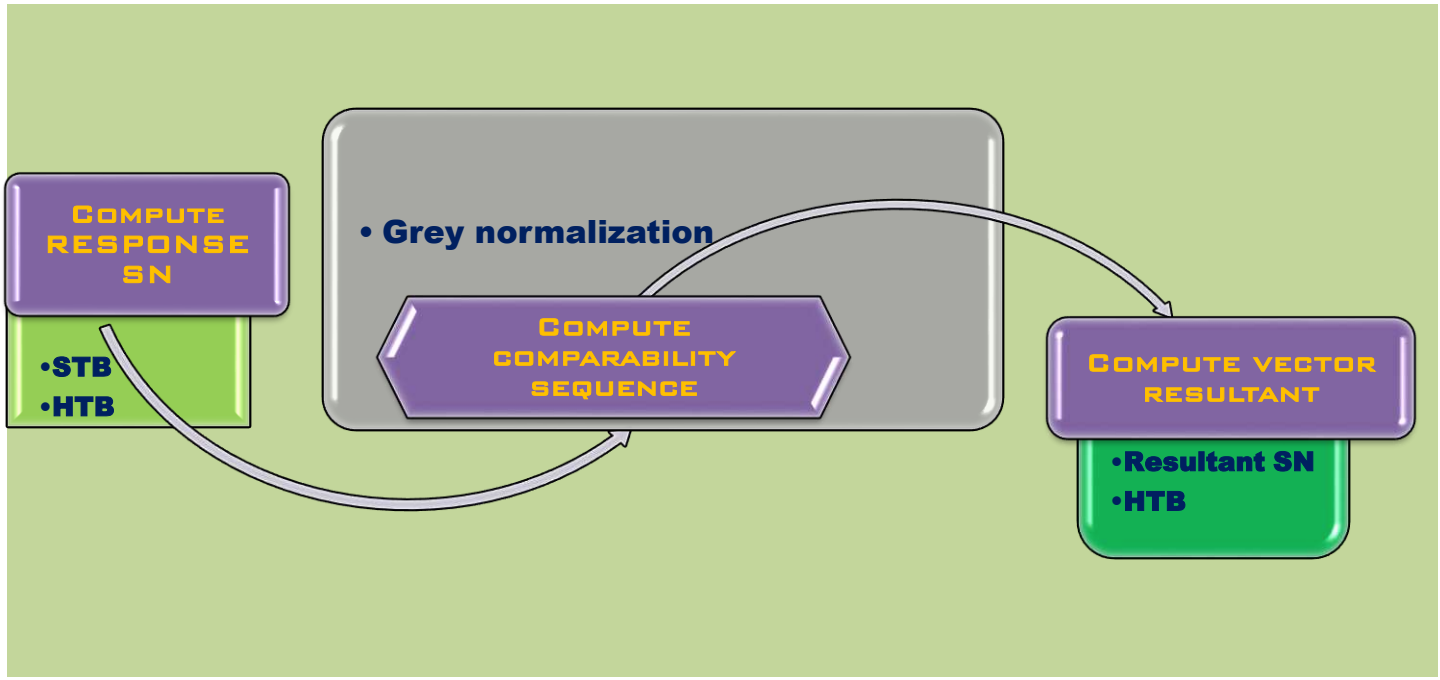


Fig 1. Flowchart for the novel multi-response optimization based on Taguchi-GVA

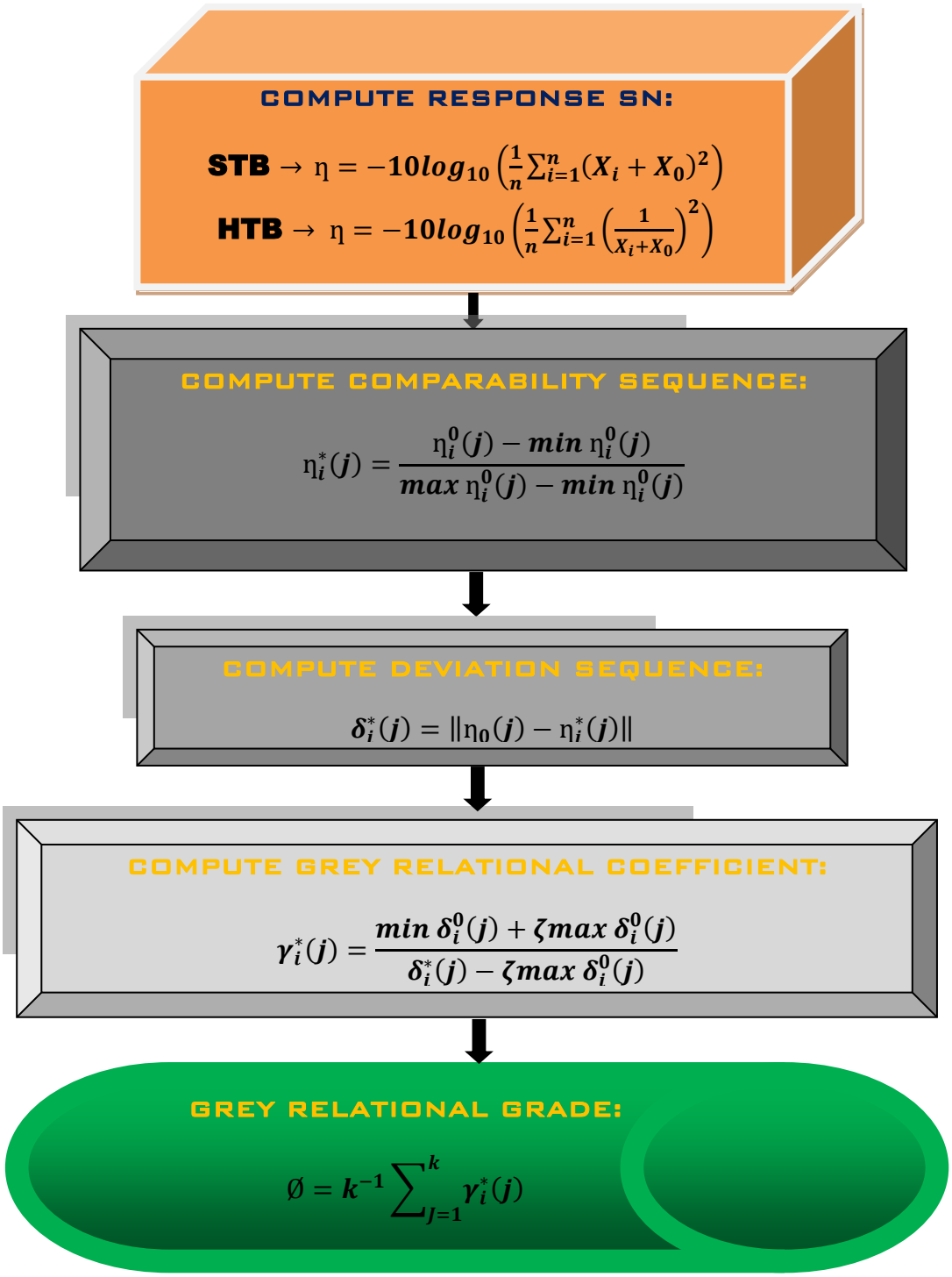


Fig 2. Flowchart for the multi-response optimization based on Taguchi-GRA

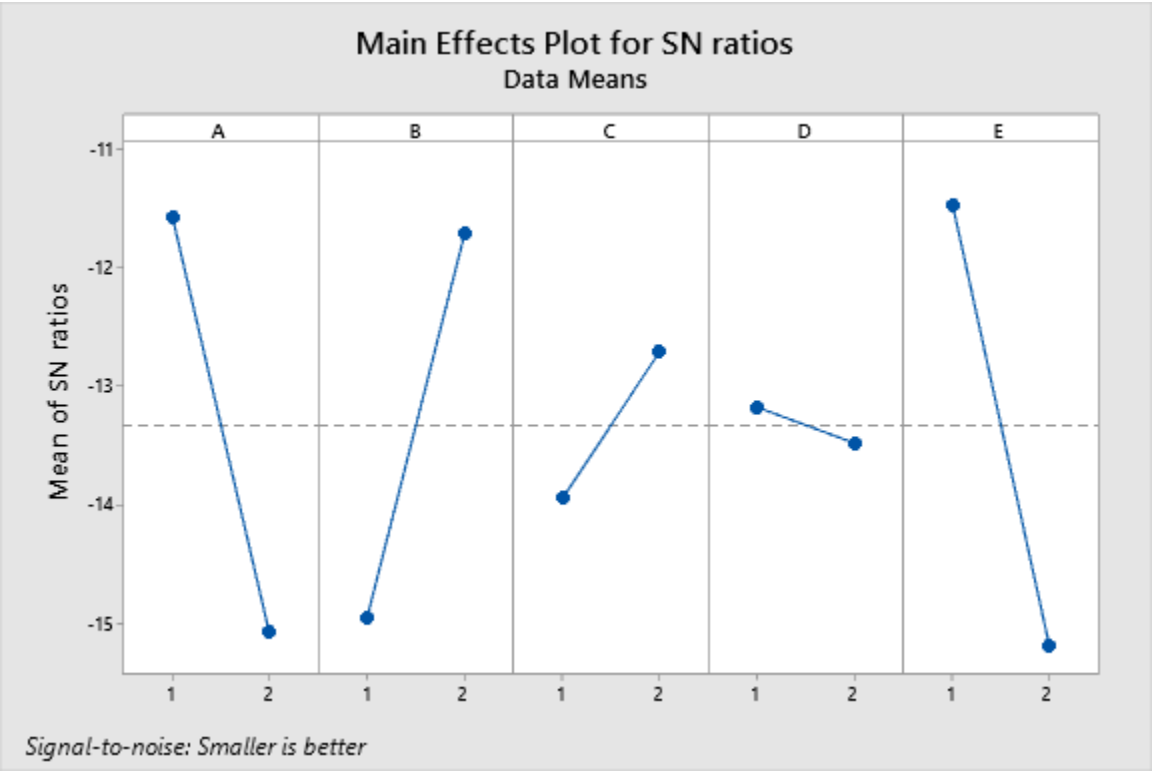


Fig 3. Plot of factor effect on the SN of DS

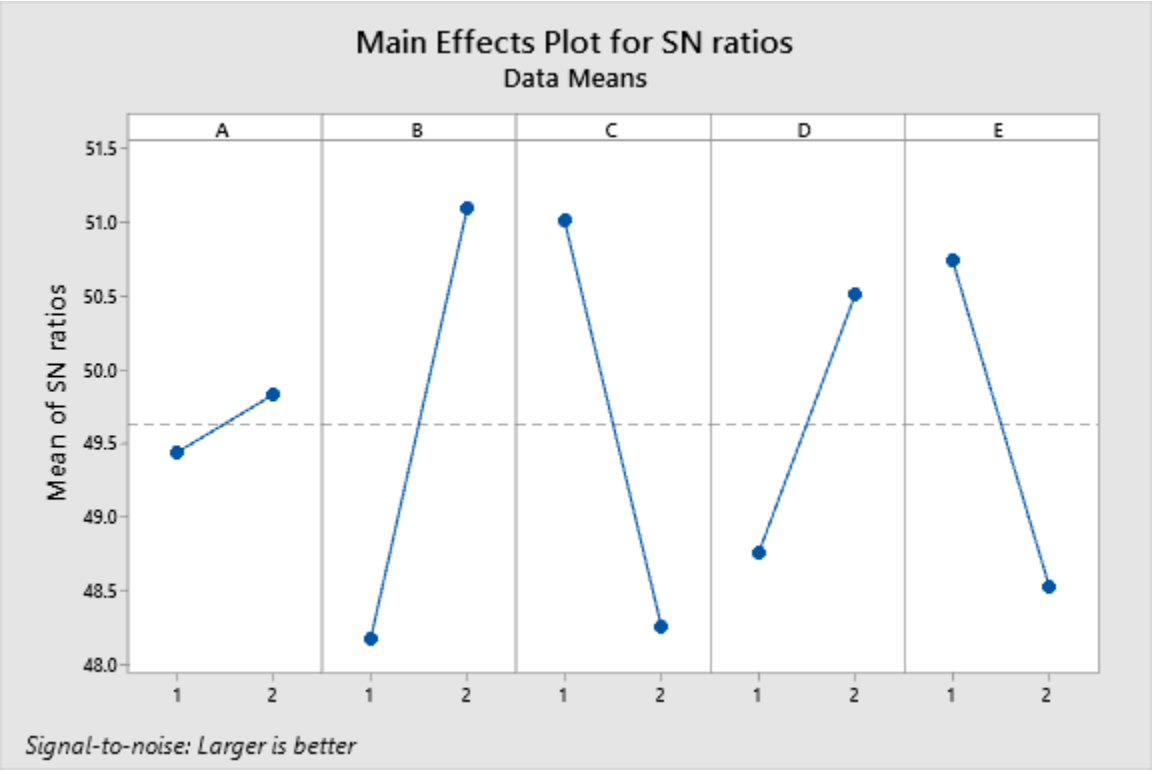


Fig 4. Plot of factor effect on the SN of UCS

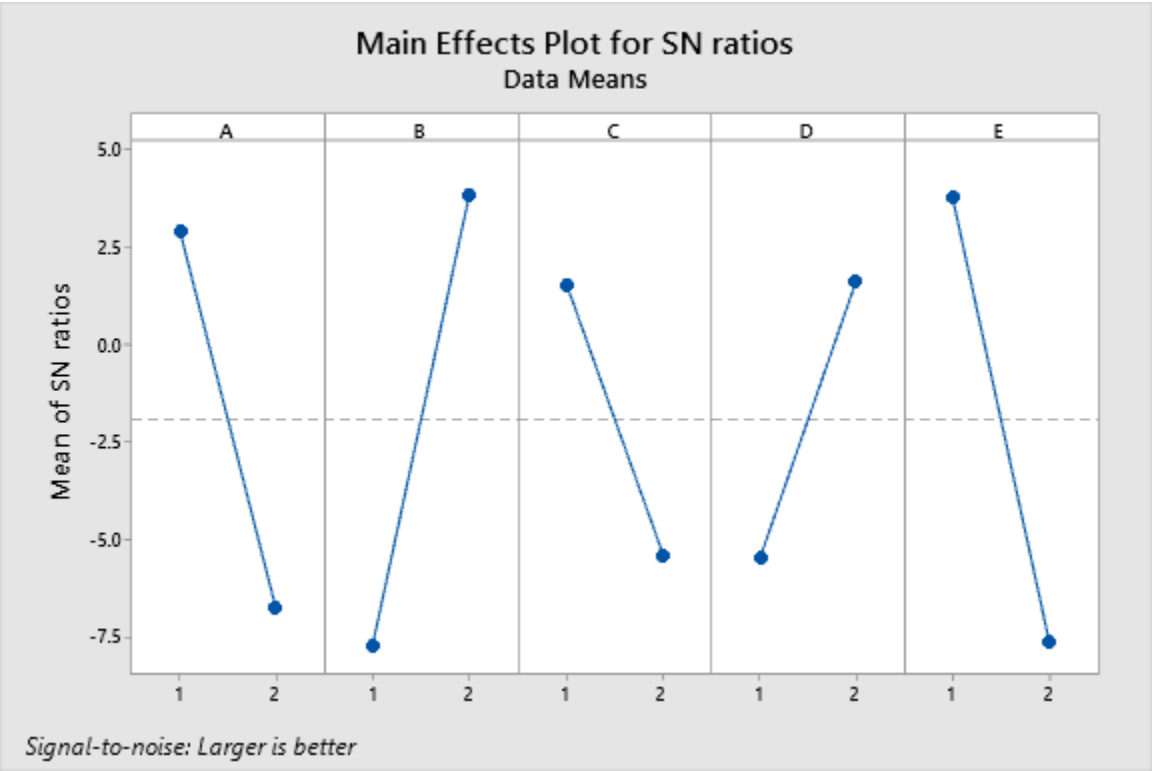


Fig 5. Plot of factor effect on the SN of vector resultant


Fig 6. Plot of factor effect on the SN of grey ordinal value

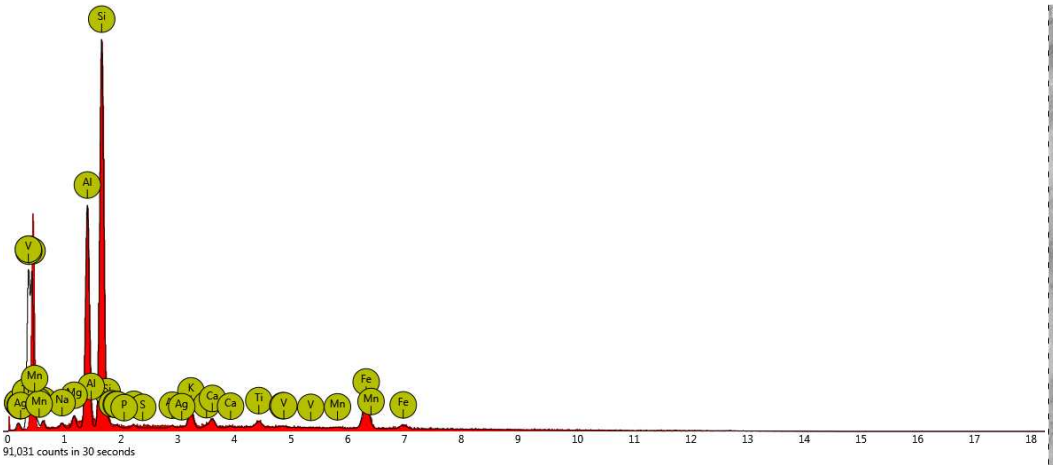


(a)

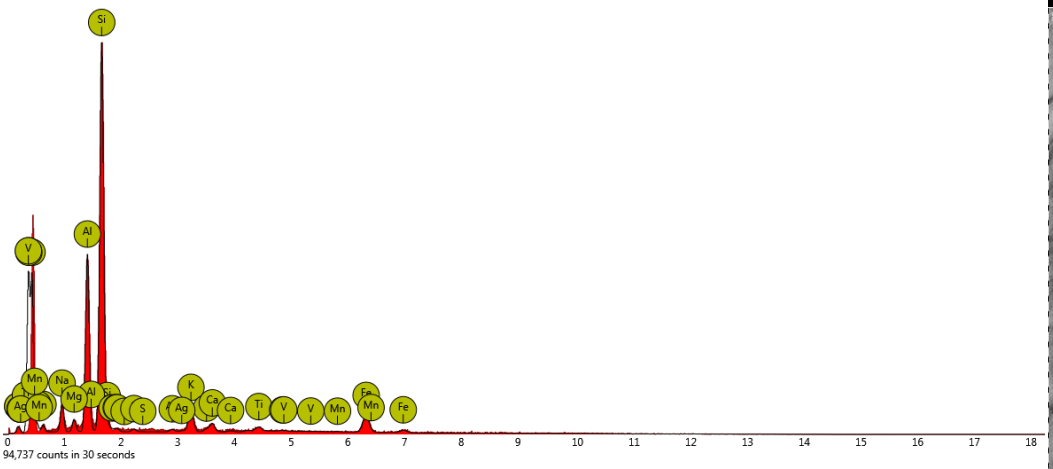


(b)

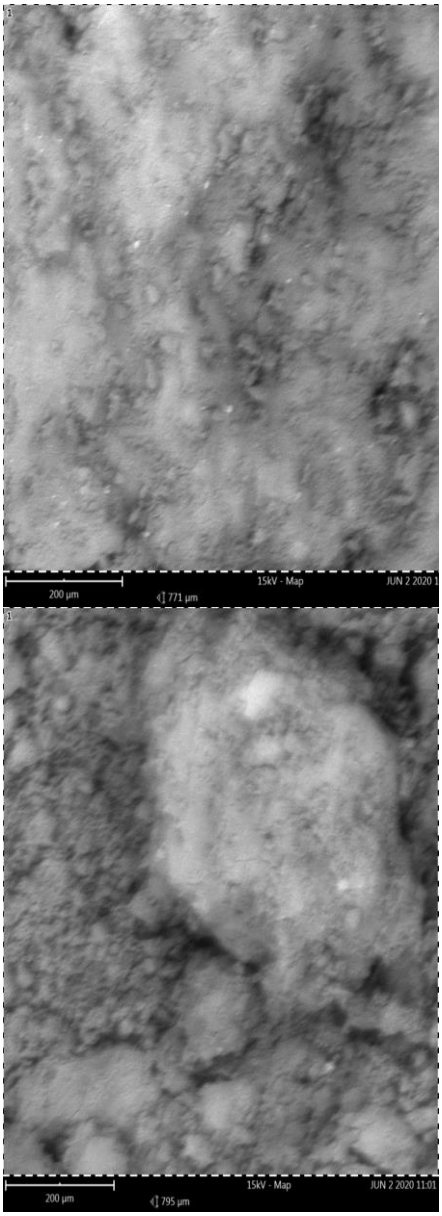


Fig 7. EDSE peaks for (a) natural soil (b) optimally stabilized soil

Table

**Table 1.** Geotechnical/physical properties of the TBC soil

| S/No | Property | Description |
|---|---|---|
| 1 | Specific gravity | 2.62 |
| 2 | Natural moisture content | 9.9% |
| 3 | Fines | 80.1% |
| 4 | Sand | 19.9% |
| 5 | Liquid limit | 66.0% |
| 6 | Plastic limit | 34.9% |
| 7 | Plasticity index | 31.1% |
| 8 | Optimum moisture content (OMC) | 19.7% |
| 9 | Maximum dry density (MDD) | 1.59g/cm$^3$ |
| 10 | AASHTO classification | A-7-5 |
| 11 | USCS classification | CH |
| 12 | Permeability | 2.025x10$^{-9}$ ms$^{-1}$ |
| 13 | UCS | 130 kN/m$^2$ |
| 14 | DS | 20.3% |

Table 2. Major oxide composition of the soil and industrial waste materials

| Compound (%) | Soil | QW | PFA |
|---|---|---|---|
| $Al_2O_3$ | 17.7 | 20.4 | 16.3 |
| $SiO_2$ | 59.3 | 50.3 | 59.8 |
| $Fe_2O_3$ | 5.4 | 0.7 | 9.6 |
| CaO | 0.8 | 1.5 | 0.8 |
| $K_2O$ | 2.1 | 2.3 | 1.2 |
| $TiO_2$ | 0.7 | 0.2 | 0.5 |
| $SO_3$ | 0.3 | <0.1 | <0.1 |
| Loss on ignition | <10 | <10 | <10 |

**Table 3.** Designation of process parameters and their levels

| Factor Designation | Level | |
|---|---|---|
| | 1 | 2 |
| **A** | PFA | QW |
| **B** | 10% | 20% |
| **C** | NaOH | KOH |
| **D** | 0.5 | 0.7 |
| **E** | M1 | M2 |

**Table 4.** Design orthogonal array with coded and uncoded variables and SN

| Run | A | B | C | D | E | A | B | C | D | E | UCS SN | DS SN |
|---|---|---|---|---|---|---|---|---|---|---|---|---|
| 1 | PFA | 10% | NaOH | 0.5 | M1 | 1 | 1 | 1 | 1 | 1 | 48.9432 | -12.041 |
| 2 | PFA | 10% | KOH | 0.7 | M1 | 1 | 1 | 2 | 2 | 1 | 49.218 | -10.63 |
| 3 | PFA | 20% | NaOH | 0.7 | M2 | 1 | 2 | 1 | 2 | 2 | 51.5957 | -13.255 |
| 4 | PFA | 20% | KOH | 0.5 | M2 | 1 | 2 | 2 | 1 | 2 | 47.9935 | -10.37 |
| 5 | QW | 10% | NaOH | 0.7 | M2 | 2 | 1 | 1 | 2 | 2 | 49.9662 | -18.69 |
| 6 | QW | 10% | KOH | 0.5 | M2 | 2 | 1 | 2 | 1 | 2 | 44.5577 | -18.486 |
| 7 | QW | 20% | NaOH | 0.5 | M1 | 2 | 2 | 1 | 1 | 1 | 53.5339 | -11.821 |
| 8 | QW | 20% | KOH | 0.7 | M1 | 2 | 2 | 2 | 2 | 1 | 51.2696 | -11.364 |

**Table 5.** Output for the multi-response GVA

| Run | Comparability sequence | | Vector resultant |
|---|---|---|---|
| | $\eta_i^*(UCS)$ | $\eta_i^*(DS)$ | Ŗ |
| 1 | 0.799 | 0.489 | 1.288 |
| 2 | 0.969 | 0.519 | 1.488 |
| 3 | 0.653 | 0.784 | 1.437 |
| 4 | 1.000 | 0.383 | 1.383 |
| 5 | 0.000 | 0.603 | 0.603 |
| 6 | 0.025 | 0.000 | 0.025 |
| 7 | 0.826 | 1.000 | 1.826 |
| 8 | 0.881 | 0.748 | 1.628 |

**Table 6.** Response table for the vector resultant HTB SN

| Level | A | B | C | D | E |
|---|---|---|---|---|---|
| 1 | 2.904 | -7.736 | 1.544 | -5.488 | 3.778 |
| 2 | -6.783 | 3.857 | -5.423 | 1.609 | -7.657 |
| Delta | 9.686 | 11.593 | 6.967 | 7.098 | 11.435 |
| Rank | 3 | 1 | 5 | 4 | 2 |

Table 7. Analysis of variance for vector resultant

| Process factor | DOF | SS | V | F-ratio | P (%) |
|---|---|---|---|---|---|
| A | 1 | 0.200 | 0.200 | 4.703 | 10.4 |
| B | 1 | 0.805 | 0.805 | 18.915 | 41.7 |
| C | 1 | 0.501 | 0.501 | 1.192 | 2.6 |
| D | 1 | 0.046 | 0.046 | 1.076 | 2.4 |
| E | 1 | 0.741 | 0.741 | 17.424 | 38.5 |
| Error | 2 | 0.085 | 0.043 | | 4.4 |
| Total | 7 | 1.927 | | | 100.0 |

**Table 8.** Output for the multi-response GRA

| Run | Deviation sequence | | Grey relational coefficient | | GRG | Ordinal values (rank) |
|---|---|---|---|---|---|---|
| | $\delta_i^*(UCS)$ | $\delta_i^*(DS)$ | $\gamma_i^*(UCS)$ | $\gamma_i^*(DS)$ | $\emptyset$ | |
| 1 | 0.201 | 0.511 | 0.713 | 0.494 | 0.604 | 3 |
| 2 | 0.031 | 0.481 | 0.941 | 0.510 | 0.726 | 6 |
| 3 | 0.347 | 0.216 | 0.590 | 0.698 | 0.644 | 4 |
| 4 | 0.000 | 0.617 | 1.000 | 0.448 | 0.724 | 5 |
| 5 | 1.000 | 0.397 | 0.333 | 0.557 | 0.445 | 2 |
| 6 | 0.975 | 1.000 | 0.339 | 0.333 | 0.336 | 1 |
| 7 | 0.174 | 0.000 | 0.741 | 1.000 | 0.871 | 8 |
| 8 | 0.119 | 0.252 | 0.807 | 0.665 | 0.736 | 7 |

**Table 9.** Euclidean distance for performance comparison

| Designation | UCS | DS | $\eta^{UCS}$ | $\eta^{DS}$ | $\Delta_{raw}$ | $\Delta_{norm}$ |
|---|---|---|---|---|---|---|
| Single response | 489.25 | 1.1 | 1 | 1 | - | - |
| Multi-response GVA | 458 | 1.85 | 0.75 | 0 | 31.2589987 | 1.03 |
| Multi-response GRA | 364.25 | 1.275 | 0 | 0.766667 | 125.0001225 | 1.03 |

**Table 10.** Summary of relevant FTIR peaks and related functional groups

| | Wave number ($cm^{-1}$) | Functional group |
|---|---|---|
| **Natural soil** | 3698, 3623, 3392, 1636 | – OH and H – O – H weakly bonded water molecules |
| | 1979, 775 | Inactive alumino-silicate sites |
| | 995, 682 | Quartz band |
| **Stabilized soil** | 3694, 3619, 3366, 1636 | H – O – H strongly bonded water molecules |
| | 2099 | Inactive alumino-silicate site |
| | 1394 | O – C – O carbonate group |
| | 999, 746 | T – O (T = Si/Al) alumino-silicate gel band, siloxo Si-O-Si alumino-silicate framework structures |

**Table 11.** Summary of atomic concentration for relevant EDSE peaks

| Element Symbol | Natural soil atomic concentration | Stabilized soil atomic concentration |
|---|---|---|
| Si | 50.1 | 51 |
| Al | 27.6 | 23 |
| Fe | 10.8 | 7.2 |
| K | 2.9 | 4.4 |
| Ti | 1.4 | 0.9 |
| Ca | 1.6 | 1.6 |
| Mg | 2.1 | 2.3 |
| Na | 1.4 | 7.7 |

Formatted Table